International Journal of Heat and Mass Transfer 54 (2011) 5109–5115

Contents lists available at ScienceDirect

International Journal of Heat and Mass Transfer

journal homepage: www.elsevier.com/locate/ijhmt

Experimental investigation for effects of a reciprocating motion on mixed convection of a curved vertical cooling channel with a heat top surface

Wu-Shung Fu *, Chung-Jen Chen, I-Chou Liu, Liang-Ying Hou

Department of Mechanical Engineering, National Chiao Tung University, 1001 Ta Hsueh Road, Hsinchu 30010, Taiwan, ROC

ARTICLE INFO

Article history:
Received 25 May 2011
Received in revised form 12 July 2011
Accepted 12 July 2011
Available online 8 August 2011

Keywords:
Reciprocating motion
Mixed convection
Experimental study

ABSTRACT

An experimental work is conducted to investigate effects of a reciprocating motion on mixed convection of a curved vertical cooling channel with a heat top surface, and numerical work is executed simultaneously to validate the experimental results auxiliarily. The experimental apparatus are composed of three main parts of a cooling channel, reciprocating movement and heating control. The working fluid is air and data runs are performed for Reynolds numbers, frequencies, amplitudes and temperature differences. Heat transfer rates are affected by cooling fluid flowing and reciprocating motion mutually. The enhancement of heat transfer rate is definite and the most achievement is about 50% in this work. Comparisons of both experimental and numerical results have good agreements.

1. Introduction

The study of dynamic motion of an equipment affecting the heat transfer of the equipment itself is very important and it is usually found out in many industrial equipments, especially in the equipments like piston, pump and compressor operated by reciprocating behaviors. Since the equipments often suffer from a high temperature situation, the mixed convection becomes an appropriate mode to be adopted to clarify the detailed heat transfer mechanisms of the equipments. Due to the importance of industrial application, in spite of viewpoints of academy or practice the study still attracts a lot of attention. Besides, the similar study of heat transfer of pulsating or oscillating flow in stationary equipment is another important issue. There are some substantial differences between the two studies though, both subjects are always lumped to be discussed together. As a results, for facilitating the analysis of the former study a simulation of pulsating or oscillating flow in a stationary channel is often equivalently adopted to substitute the analysis of the former study. The relating literature was published in [1–9]. However, main characteristics of the study mentioned formerly are caused by that when cooling fluids flowing through the dynamic equipment interact with the reciprocating motion generated by the dynamic equipment. The phenomena are much different from those caused by a pulsating or oscillating flow in the stationary equipment. Due to the mutual interaction between the fluid flowing and reciprocating motion, both flow and thermal fields in the equipment vary periodically and become dynamic phenomena. Relatively few related literature are published.

In the past, Chiu and Kuo [10] investigated turbulent heat transfer and predicted wall heat flux in reciprocating engine by using an algebraic grid generation technique. The results showed that increasing the curvature of the cylinder head would increase the strength of induced squish flow and wall heat flux. Chang and Su [11] conducted an experimental work to investigate influence of reciprocating motion on heat transfer inside a ribbed enclosure and showed that at the highest reciprocating speed the heat transfer was enhanced about 145% of the equivalent stationary case. Chang and Su [12] modified the experiment and gained the results which at a pulsating number of 10.5, the time average Nusselt number could reach about 165% of the stationary one. Cheng and Hung [13] developed a solution method for predicting unsteady flow and thermal fields in a reciprocating piston-cylinder assembly. The results showed that the two-stage pressure correction procedure could be readily incorporated into existing numerical techniques to yield reasonably accurate results. Afterward, Chang et al. [14] set an anti-gravity open thermosyphon system and effects of inertia, pulsating and buoyancy forces were taken into consideration. A correlation formula which was consistent with the heat transfer physics expressed with dimensionless temperature was proposed. Fu et al. [15] conducted an experimental work of mixed convection in a curved channel subject to a reciprocating motion caused by the curved channel itself to simulate the heat transfer of a piston. In the study, an object in which a heat bottom surface was installed in the curved channel and both directions of inlet fluid flowing and buoyancy force were opposite was studied.

* Corresponding author. Address: Department of Mechanical Engineering, National Chiao Tung University, 1001 Ta Hsueh Road, Hsinchu 30056, Taiwan. Tel.: +886 3 5712121x55110; fax: +886 3 5720634.
E-mail address: wsfu@mail.nctu.edu.tw (W.-S. Fu).

0017-9310/$ - see front matter © 2011 Elsevier Ltd. All rights reserved.
doi:10.1016/j.ijheatmasstransfer.2011.07.030

Nomenclature

A	area [m^2]
f_c	frequency [s^{-1}]
F_c	dimensionless frequency [$F_c = wf_c/v_0$]
Gr	Grashof number [$Gr = g\beta(T_w - T_\infty)w^3/v^2$]
h	heat transfer coefficient [W m^{-2} K^{-1}]
I	current [A]
k	thermal conductivity [W m^{-1} K^{-1}]
K	Kelvin temperature
l	length of linking bar [m]
l_c	length from linking bar to shaft [m]
L_c	dimensionless amplitude [$L_c = l_c/w$]
Nu	Nusselt number (Eq. (4))
Q	heat energy [W]
Re	Reynolds number ($\rho v_0/v$)
ΔT	temperature difference [K]
v_c	velocity of reciprocating channel [m s^{-1}]
v_0	average velocity of air stream [m s^{-1}]
V	voltage [V]
w	width of channel [m]
Δy	thickness of basswood [m]

Greek symbols

v	kinematics viscosity [m^2 s^{-1}]
ρ	Density [kg m^{-3}]
τ	dimensionless time [$\tau = tv_0/w$]

Subscripts

b	basswood
h	heater
in	input
$loss$	loss
w	wall

Parameters of Reynolds number, temperature difference, and frequency were considered and the maximum enhancement of heat transfer was about 35%. In this situation, the arrangement of installation of a heat bottom surface in the curved channel was advantages to heat transfer rate. However, from a view point of heat transfer, a situation of installation of a heat top surface in the curved channel in which both directions of inlet cooling fluid flowing and buoyancy are the same and the thermal stratification layer tightly attaches to the heat surface is inferior to the former situation, and scarcely studied beforehand. Therefore, the clarification of phenomena of the latter situation will be profitable to improve heat transfer and avoid heat damage of it.

The aim of this study investigates effects of a reciprocating motion on mixed convection of a curved vertical channel with installation a heat top surface experimentally. Numerical calculations are executed auxiliarily to validate the experimental results. The apparatus used in this study include a cooling channel, reciprocating and heating control systems. The cooling channel system which is composed of a fan, a volume flow meter, two fixed channels and a reciprocating channel provides a designed flow velocity and unites a curved shape channel. The reciprocating system which plays a role maintains a reciprocating motion of the curved shape channel smoothly and steadily. The heating control system is combined with numerous heaters, power supplies and thermocouples, and it holds a constant surface temperature condition on the heaters. Parameters of Reynolds numbers, frequency, amplitudes and temperature difference are examined, and the range of Gr/Re^2 varies from 0.8 to 6.47. The consistence gives good agreement for comparing both the numerical and experimental results.

2. Physical model and experimental procedure

A curved cooling channel used in this study is shown in Fig. 1, and the related experimental apparatus which include three main systems of a cooling channel system (5), reciprocating system (4) and heating control system (6,7).

In the cooling system, air streams flowing through the cooling channel (5) are suck by a fan (1) and the volume flow rate of air streams is measured by a flow meter (2) for calculating the average velocity of air streams which is used to compute Reynolds number. For rectifying the air streams, a honey comb (3) is installed in the entrance of the cooling channel. The cooling channel is set vertically and composed of a reciprocating channel (51), two fixed channels (52) and two connecting channels (53). The reciprocating channel is set on the reciprocating system (4) to execute reciprocating motion.

In Fig. 2a, the cooling channel is made of rectangular ducts of which the height and width are 120 mm and 30 mm, respectively. The connecting channel (53) connects the reciprocating (51) and fixed (52) channels. To avoid leakage of the air streams and improve smoothness of reciprocating motion of the reciprocating channel, the tolerance between the connecting channel and both the reciprocating and the fixed channels is filled with grease. v_0 is the average velocity of cooling fluids, and v_c is the reciprocating velocity of the reciprocating channel (51). Three heat regions of front, middle and back are sequentially arranged along the air streams flow, and the detailed dimensions are indicated in Fig. 2b.

Shown in Fig. 3a, the reciprocating system includes a stepping motor (41), a rotating circular plate (42), linkage bar (43), pedestal (44), pair of tracks (45), and pair of sliders (46). The stepping motor

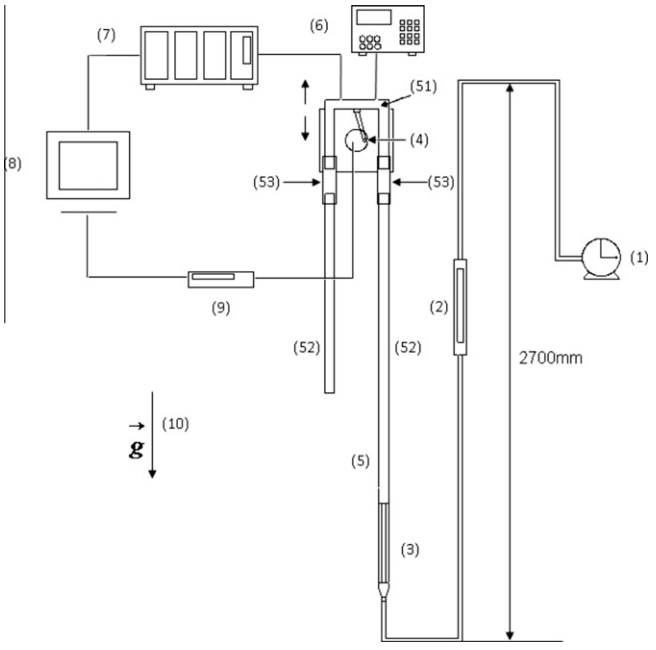

Fig. 1. Experimental apparatus.

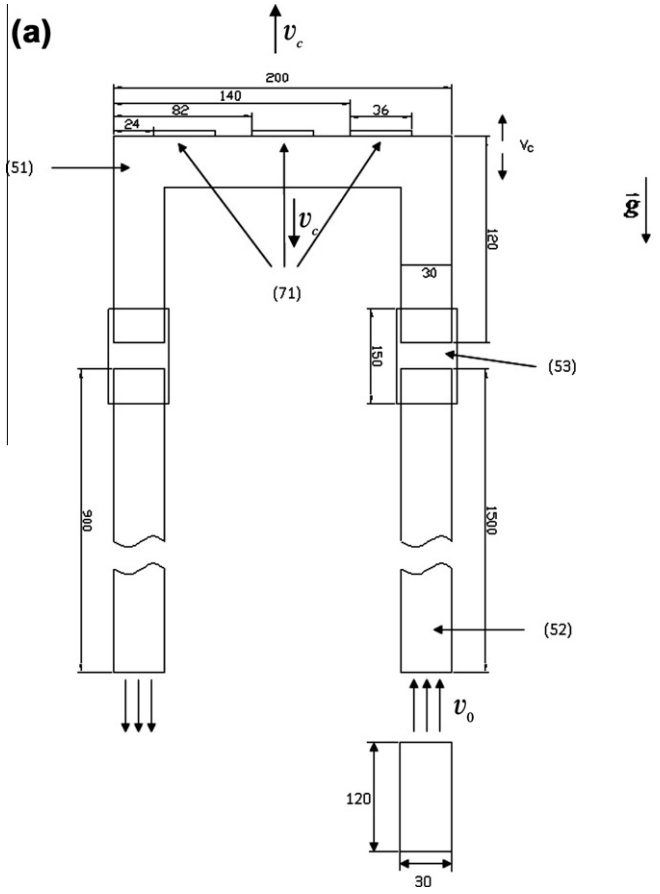

Fig. 2a. Dimensions of cooling channel.

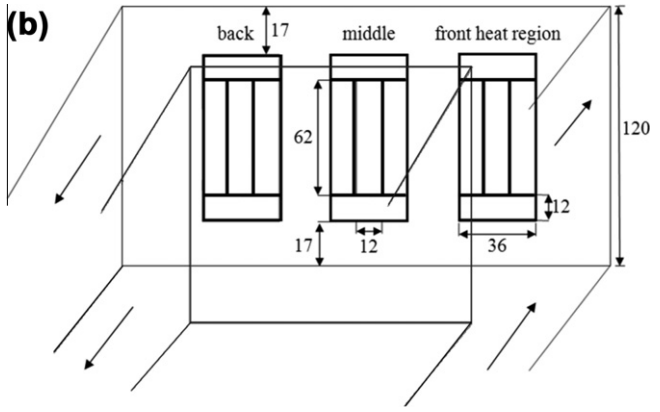

Fig. 2b. Dimensions of each heat region.

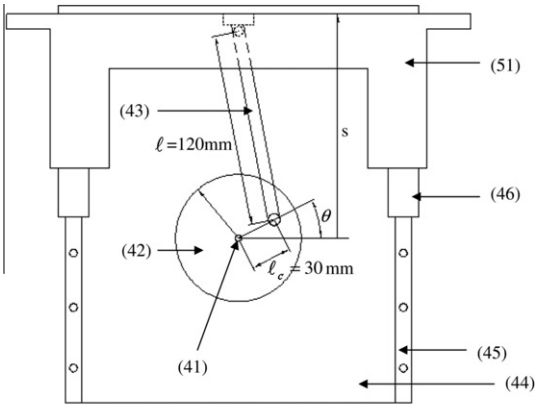

(41) motor transmission shaft
(42) rotating circular plate
(43) linking bar
(44) pedestal
(45) track
(46) slider
(51) reciprocating channel

Fig. 3a. Reciprocating system.

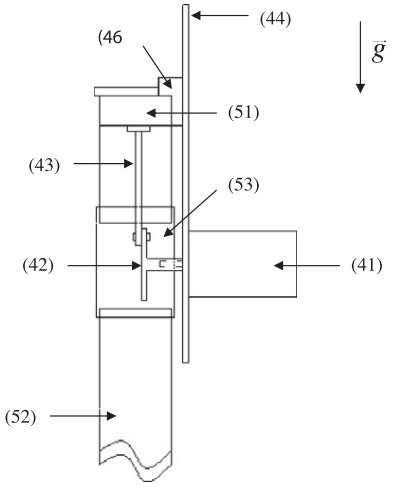

(41) stepping motor
(42) rotating circular plate
(43) linking bar
(44) pedestal
(46) slider
(51) reciprocating channel
(52) fixed channel
(53) connecting channel

Fig. 3b. Combination of cooling channel system and reciprocating system.

(41) installed below the pedestal (44) leads the rotating circular plate (42) to rotate, and via the linking bar (43) brings the sliders to move reciprocally. The rotating speed used for marine engine is slow, based on the information of Sulzer [16], the maximum frequency adopted in this work is 2/s. Since the reciprocating channel is set on the sliders shown in Fig. 3b, the reciprocating channel could move with the sliders synchronously, and meets the demand of reciprocating movement.

The heat control system is composed of heat regions, thermocouples, temperature indicators and power supplies. The heater structure is indicated in Fig. 4 and the main heater (712) of each region is adapted to measure heat transfer rate. The heat transfer rate of the mixed convection is small, and the prevention of the heat dissipation by a heat conduction mode from the main heater becomes important. Then the other four heaters ((711), (713), (714), and (715)) set around the main heater are used as guard heaters to prevent the heat dissipation from the main heater. In order to maintain a constant wall temperature condition on each heater, each heater is individually controlled by a power supply which is a direct current mode. As for the manufacturing of the heater, numerous small holes are drilled uniformly on a thin insulated material such as PCB (71), and a fine Ni–Cr line 0.1 mm (72) in diameter which is regarded as a heater during electrical power applying on threads pierces through the holes tightly. A thin copper plate (74) covers the heater completely, and for prohibiting the copper plate to contact the Ni–Cr line directly two thick pieces of Teflon tape (73) are separately interpreted into both places between the copper plate and heater. Eighteen thermocouples (77) indicated by × signal stuck on each copper plate are used to

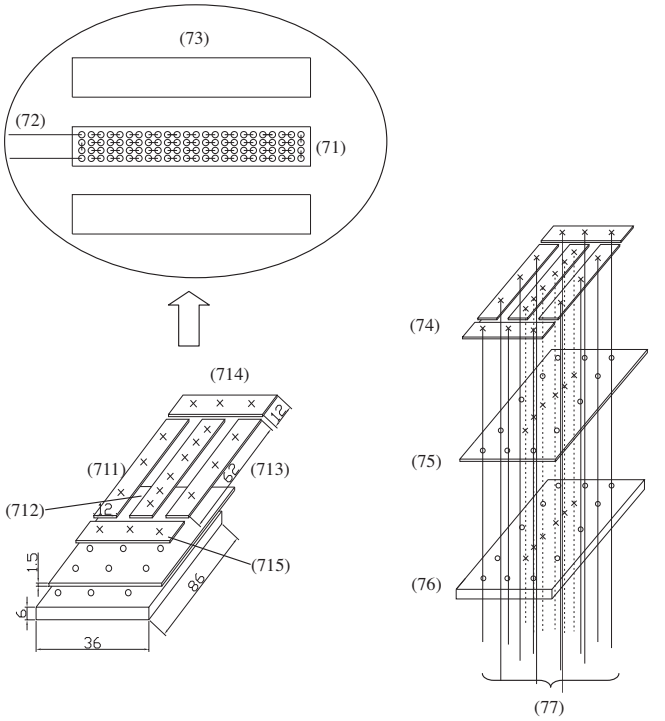

(71) heater
(72) Nickel-Chromium alloy wire
(73) Teflon tape
(74) thin cooper plate
(75) 1.5mm basswood
(76) 6mm basswood
(77) thermocouples
(711) guard heater
(712) main heater
(713) guard heater
(714) guard heater
(715) guard heater

Fig. 4. Heater structure.

measure the temperatures of heater. Besides, a block of thin basswood (1.5 mm) is used to estimate heat dissipation by heat conduction from the bottom surface of the heater. Twelve thermocouples are then evenly installed on both surfaces of the thin basswood. A diameter of thermocouples is about 0.2 mm. Below the thin basswood, a block of thick basswood (6 mm) is set to prevent heat dissipation further.

Each result is obtained by an average magnitude of three experimental runs and a brief outline is given as follows.

(1) Start the fan to obtain the volume flow rate $\dot{Q}$ by reading the flow meter and the average velocity v_0 of the air streams by dividing the volume flow rate $\dot{Q}$ by the cross section area of cooling channel. Calculate the following equation to obtain the Reynolds number Re .

$$\mathrm{Re} = \frac{v_0 w}{v} \tag{1}$$

(2) Select a designed revolution of the stepping motor to obtain the frequency f_C.
(3) Apply the power supply on the corresponding heater. Adjust the amount of electric power of power supply to obtain the designed temperature of heater.
(4) Calculate the heat transfer rate of middle heater by the following equations.
(a) Total input heat energy

$$Q_{in} = I \times V \tag{2}$$

where Q_{in} is the total input heat energy, I and V are current and voltage of electric power, respectively.

Table 1
Parameters conducted in experimental runs.

	$\mathrm{Re_w}$	$Gr/\mathrm{Re_w}^2$	ΔT_w (°C)	F_c	L_c
Case 1	300	0.4	10	0	0
Case 2	300	1.62	40	0	0
Case 3	200	0.91	10	0	0
Case 4	200	3.64	40	0	0
Case 5	300	0.4	10	0.2	1.0
Case 6	300	1.62	40	0.4	1.0
Case 7	300	1.62	40	0.4	0.75
Case 8	200	0.91	10	0.2	1.0
Case 9	200	3.64	40	0.4	1.0

Table 2
Uncertainty analyses of front heat region under Re = 300.

Parameter	Uncertainty
$\mathrm{Re_w}$	±1.78%
Nu	±3.68%
$Gr/\mathrm{Re_w}^2$	±4.53%

(b) Heat dissipation Q_{loss} from the basswood installed on the bottom side of the heater.

$$Q_{loss} = k_b \times A_b \times \Delta T_b / \Delta y \tag{3}$$

where k_b is the thermal conductivity of basswood (≒0.055 W/(m K)), A_b is the area of basswood below the middle heater, ΔT_b (K) is the temperature difference between the upper and bottom sides of basswood, and Δy is the thickness of basswood (≒1.5 mm).

(c) Average Nusselt number Nu of the middle heater.

$$Nu = \frac{hw}{k} = \frac{Q_{conv}}{A_h \cdot \Delta T_w} \cdot \frac{w}{k} \tag{4}$$

$$Q_{conv} = Q_{in} - Q_{loss} \tag{5}$$

where Q_{conv} is heat energy brought by air stream flow, A_h is area of a heater, w is width of cooling channel, ΔT_w (K) is temperature difference between heater surface and environment. k is thermal conductivity of air.

During the calculating processes, an average temperature which means the average magnitude of all the temperatures of thermocouples installed on the heater is not more than individual temperature of thermocouple of 0.3 °C, and used to calculate the heat transfer rate of each experimental run.

Situations conducted in this study are indicated in Table 1. According to the data of marker, the resolutions of thermocouple and temperature instruments are 0.1 °C and 0.75%, respectively. The uncertain analyses are based on Kline [17], the related uncertainties of one situation are tabulated in Table 2.

For validating the experimental results, a numerical method is executed auxiliarily. Corresponding to the main part of experimental apparatus, three dimensional physical model is simulated, the computing conditions of $k-\varepsilon$ turbulent model and 1% turbulence intensity at the inlet are adopted. The code of STAR-CD is adopted to execute the computing processes. The grid distributions of the reciprocating channel are denser than these of both fixed channels, and the total grid number is about 600,000.

3. Results and discussion

Shown in Table 3, there are surface temperatures of front (F), middle (M) and back (B) heat regions, respectively. Most of the temperature differences which mean the deviations between local temperatures and average temperature are smaller than 0.3 °C, the

Table 3
Local temperature distributions (Re = 300).

42.7 °C	42.8 °C	42.6 °C (4)	42.5 °C	42.8 °C	42.8 °C	42.6 °C	42.7 °C	42.5 °C
	42.7 °C			42.8 °C			42.7 °C	
42.7 °C		42.7 °C	42.7 °C		42.9 °C	42.6 °C		42.6 °C
	42.7 °C			42.9 °C			42.6 °C	
	42.8 °C			43.0 °C			42.8 °C	
42.6 °C		42.6 °C	42.6 °C		42.8 °C	42.5 °C		42.7 °C
	42.8 °C			42.8 °C			42.8 °C	
42.5 °C		42.5 °C		42.9 °C			42.7 °C	
	42.7 °C		42.6 °C		42.8 °C	42.6 °C		42.7 °C
(1)	(2)	(3)		42.8 °C			42.7 °C	
42.5 °C	42.8 °C	42.7 °C (5)	42.8 °C	42.6 °C	42.7 °C	42.6 °C	42.7 °C	42.5 °C
$F(\overline{42.7}$ °C)			$M(\overline{42.7}$ °C)			$B(\overline{42.6}$ °C)		

uniformity of temperature distributions of each region is available, the designation of the constant wall temperature condition is validated.

In Fig. 5, under the same condition the results of three experimental runs and numerical results are shown. The locations of the characters of F, M and B separately indicate the relative positions of front, middle and back heat regions installed in the horizontal channel. The maximum deviation among the experimental results is less than 5%, the functions and stability of the apparatus are credible. Since the existing experimental results of this subject are scarcely found out, the numerical computation is auxiliarily executed to validate the accuracy of the experimental results qualitatively. The maximum deviation occurring at the front region between both experimental and numerical results is less than 15%.

Shown in Fig. 6, the Nusselt numbers of the front, middle and back heat regions under different frequency situations are indicated. The magnitude of Gr/Re^2 is 0.4 which means the forced convection to dominate the heat transfer mechanism. Since the cooling fluids first impinge on the front heat region that causes the Nusselt number of this region to be much larger than those of the other two regions. Sequentially, the cooling fluids flow over the middle heat region similar to flowing over a flat plate, the Nusselt number is naturally decreased compared with that of the former region, and the magnitude of Nusselt number is fair. Because the location of the back heat region is close to the corner region and the cooling fluids turn the flowing direction from horizontal to downward direction near the corner region. A circulation zone is easily formed in this region. As a result, the Nusselt number of the back heat region gets worse.

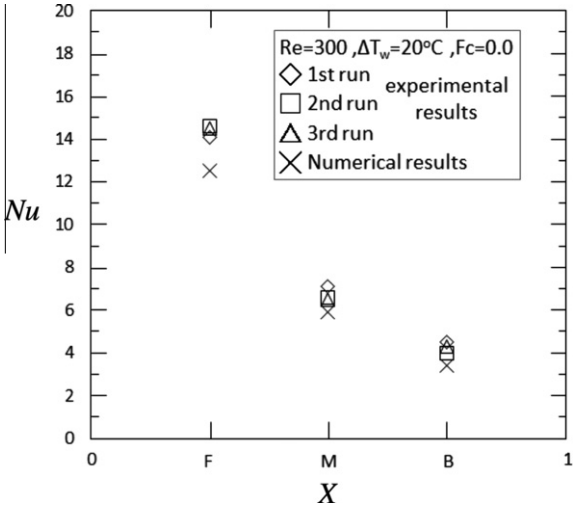

Fig. 5. Validation of reliability of experimental apparatus and consistence of experimental and numerical results.

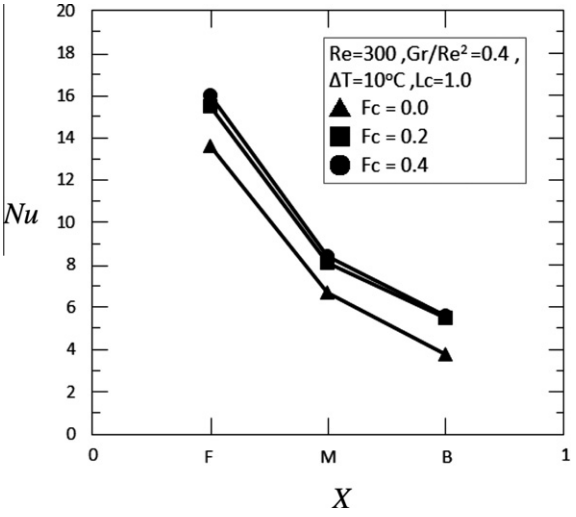

Fig. 6. Distributions of Nusselt numbers under different frequencies.

The Nusselt numbers of the situation subject to reciprocating behaviors ($F_c > 0$) are generally larger than those of the stationary state ($F_c = 0$). The enhancement of heat transfer rate of the channel caused by the reciprocating motion is definite. The thermal stratification layer attached to the top heat surface disturbed by the reciprocating motion is suggested as the main reason. Besides, the directions of both fluid flowing and reciprocating motion are vertical that causes the disturbance effects induced by different frequencies to be similar. Then the difference of the Nusselt numbers of the different frequency situations is slight.

In Fig. 7, the temperature difference ΔT increases to 40 °C and the magnitude of Gr/Re^2 becomes 1.62 that means the natural convection to play a role of the heat transfer rate. The trend of heat transfer phenomena is similar to that of previous situation shown in Fig. 6. However, at $F_c = 0.2$ situation the Nusselt number of middle heat region is decreased more drastically than that of $F_c = 0.4$ situation. And the magnitude is even almost equal to that of $F_c = 0$ situation that indicates the effect of reciprocating motion on the heat transfer rate to be nearly neglected. Since the location of middle heat region is at the center of horizontal channel far away from the inlet of horizontal channel. The influence of inlet fluid flowing on the heat transfer rate of middle heat region is not remarkable. In addition to the thermal stratification layer attached to the top heat surface of this situation is more stable than that of the previous situation, and the directions of both fluid flowing and reciprocating motion are vertical. Therefore, the situation of smaller reciprocating motion ($F_c = 0.2$) has difficulty to contribute heat transfer enhancement to the middle heat region.

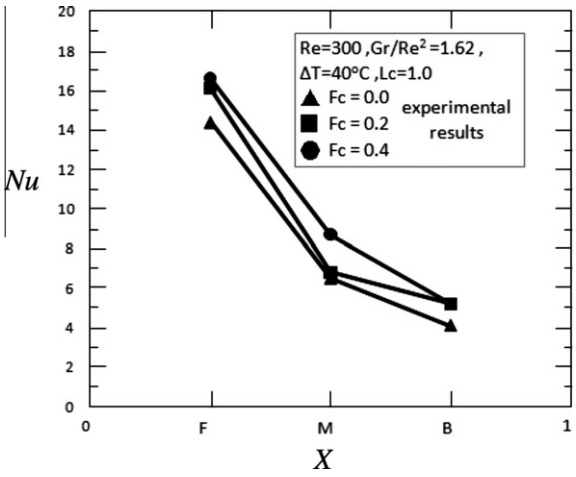

Fig. 7. Distributions of Nusselt numbers under different frequencies.

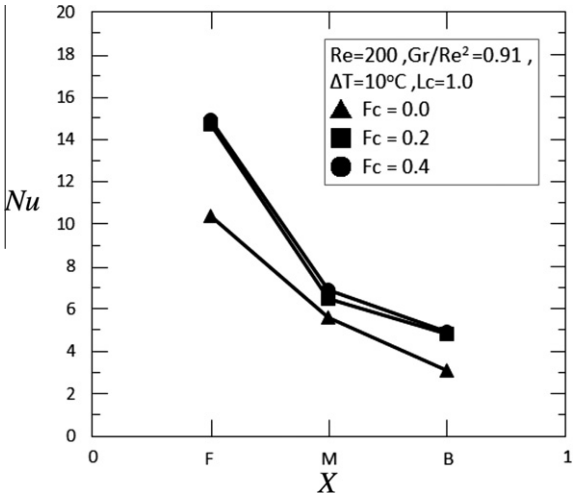

Fig. 8. Distributions of Nusselt numbers under different frequencies.

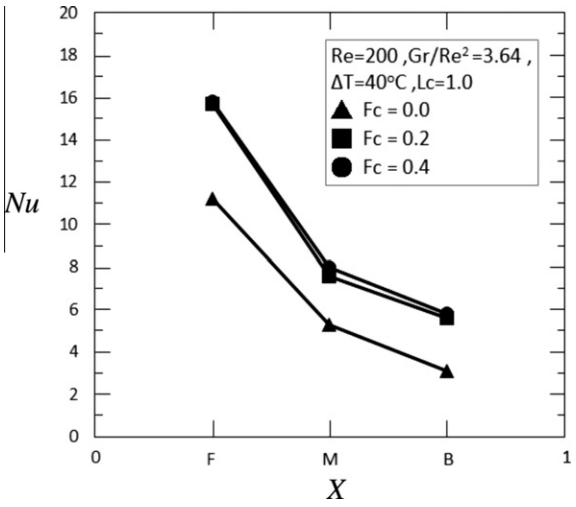

Fig. 9. Distributions of Nusselt numbers under different frequencies.

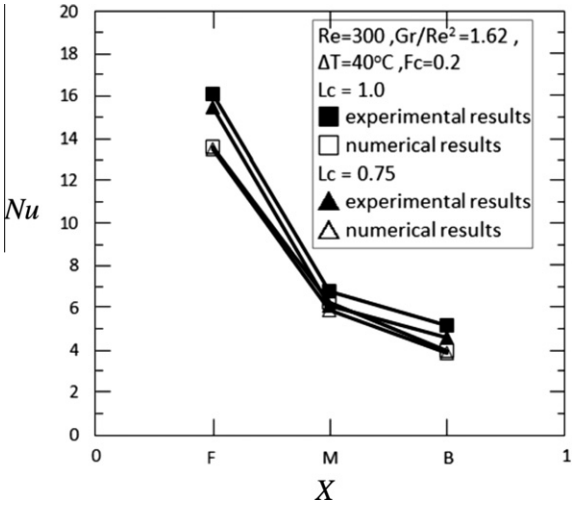

Fig. 10. Distributions of Nusselt numbers under different amplitudes.

In Fig. 8, the magnitude of Reynolds number becomes 200 that means the impulse of cooling fluids to decrease and the contribution of forced convection to the heat transfer rate of each heat region to be inferior. At the front heat region, since the impingment effect of cooling fluids still appears that causes the Nusselt number of this region to be superior to those of the other two regions. However, relative to the Nusselt number of the front region the Nusselt number of the middle region is decreased more drastically than that shown in Fig. 7, and the reason is mentioned above. The Nusselt number of the back region is still the worst, but the difference between both middle and back regions is contracted. Compared with the stationary situation ($F_c = 0$), the contribution of reciprocating motion to enhancement of heat transfer of each heat region is still remarkable.

Shown in Fig. 9, the temperature difference ΔT increases to 40 °C that means the natural convection to become strong. Then the Nusselt number of each heat region is slightly larger than that of the corresponding situation shown in Fig. 8.

In Fig. 10, the comparisons of Nusselt numbers with both experimental and numerical results under different dimensionless amplitude situations are indicated. Generally the longer the amplitude is, the effect of amplitude on the heat transfer rate becomes stronger. Then the Nusselt number of $L_c = 1.0$ situation are larger than those of $L_c = 0.75$ situation. The deviations between experimental and numerical results under different amplitude situations are similar, and the maximum deviation found out in the front heat region is about 15%. The phenomenon of numerical results decreasing drastically in the middle region is similar to that of experimental results mentioned in Fig. 7.

Shown in Fig. 11, the enhancements of heat transfer rate caused by reciprocating motions are indicated. The definition of the enhancement En (%) is shown as follows.

$$\mathrm{En} = \frac{Nu_{\text{with reciprocating motion}} - Nu_{\text{stationary state}}}{Nu_{\text{stationary state}}} \tag{6}$$

The heat transfer rate is enhanced by the reciprocating motion definitely. The larger the frequency is, the larger En (%) is achieved. Since the directions of fluid flowing and reciprocating motion are vertical, the contributions of flow flowing and reciprocating motion to the heat transfer rate are mutually affected. Consequently, under Re = 300 situation the smaller the magnitude of Gr/Re^2 is, the larger En (%) is gained. Under Re = 200 situation, the smaller the magnitude of Gr/Re^2 is, oppositely the smaller En (%) is observed. The magnitudes of En (%) of Re = 200 situation are relatively larger than those of Re = 300 situation that indicates under low Reynolds number situation the contribution of reciprocating

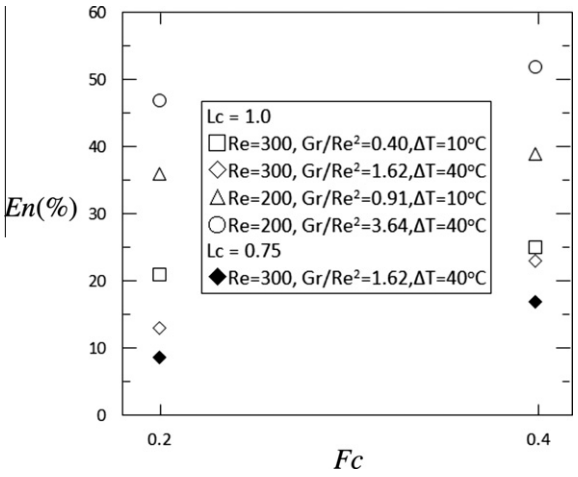

Fig. 11. Comparisons of enhancement of heat transfer rate under different parameters.

motion to the heat transfer rate to be more remarkable. The long amplitude situation is usually advantageous to the heat transfer rate, and the longer the amplitude is, the larger En (%) is achieved.

4. Conclusions

The effects of reciprocation motion on the mixed convection of curved channel with a heat top surface are conducted experimentally. The parameters of Reynolds number, frequency, amplitude and temperature difference are validated. Several conclusions are drawn as follows.

(1) The enhancement of heat transfer rate caused by the reciprocating motion is remarkable, and the maximum magnitude of enhancement is about 50% in this work.
(2) Due to mutual interaction between the fluid flowing and reciprocating motion, the enhancement achieved in the situation of Re = 200 is relatively larger than that achieved in the situation of Re = 300.
(3) The effect of reciprocating motion on the heat transfer is remarkable in the long amplitude situation, the heat transfer rate of the situation L_c = 1.0 is then larger than that of the situation of L_c = 0.75.

Acknowledgements

The support of this study by the National Science Council of Taiwan, ROC, under Contact NSC97-2221-E-009-144-MY2 and ACME-WELL Technology Co., Ltd. is gratefully acknowledged.

References

[1] P.P. Grassmann, M. Tuma, Applications of the electrolytic method-II mass transfer within a tube for steady, oscillating and pulsating flows, Int. J. Heat Mass Transfer 22 (1979) 799–804.
[2] A.T. Patera, B.B. Mikic, Exploiting hydrodynamic instabilities resonant heat transfer enhancement, Int. J. Heat Mass Transfer 29 (1986) 1127–1138.
[3] S.Y. Kim, B.H. Kang, A.E. Hyun, Heat transfer in the thermally developing region of a pulsating channel flow, Int. J. Heat Mass Transfer 36 (1993) 1257–1266.
[4] T. Nishimura, N. Kojima, Mass transfer enhancement in a symmetric sinusoidal wavy-walled channel for pulsatile flow, Int. J. Heat Mass Transfer 38 (1995) 1719–1731.
[5] T. Nishimura, A. Taurmoto, Y. Kawamura, Flow and mass transfer characteristics in wavy channels for oscillatory flow, Int. J. Heat Mass Transfer 38 (1987) 1007–1015.
[6] T. Nishimura, S. Arakawa, D. Murakami, Y. Kawamura, Oscillatory flow in a symmetric sinusoidal wavy-walled channel at intermediate Strouhal numbers, Chem. Eng. Sci. 46 (1991) 757–771.
[7] T. Nishimura, S. Arakawa, D. Murakami, Y. Kawamura, Oscillatory viscous flow in symmetric sinusoidal wavy-walled channels, Chem. Eng. Sci. 44 (1989) 2137–2148.
[8] C. Sert, A. Beskok, Oscillatory flow forced convection in micro heat spreaders, Numer. Heat Transfer Part A 42 (2002) 685–705.
[9] A.R.A. Khaled, K. Vafai, Heat transfer and hydromagnetic control of flow exit conditions inside oscillatory squeezed thin films, Numer. Heat Transfer Part A 43 (2003) 239–258.
[10] C.P. Chiu, Y.S. Kuo, Study of turbulent heat transfer in reciprocating engine using as algebraic grid generation technique, Numerical Heat Transfer Part A 27 (1995) 255–271.
[11] S.W. Chang, L.M. Su, Influence of reciprocating motion on heat transfer inside a ribbed duct with application to piston cooling in marine diesel engines, J. Ship Res. 41 (1997) 332–339.
[12] S.W. Chang, L.M. Su, Heat transfer in a reciprocating duct fitted with transverse ribs, Exp. Heat Transfer 12 (1999) 95–115.
[13] C.H. Cheng, C.K. Hung, Numerical predictions of flow thermal fields in a reciprocating piston-cylinder assembly, Numer. Heat Transfer Part A 38 (2000) 397–421.
[14] S.W. Chang, L.M. Su, W.D. Morris, T.M. Liou, Heat transfer in a smooth-walled reciprocating anti-gravity open thermosyphon, Int. J. Heat Mass Transfer 42 (2003) 1089–1103.
[15] W.S. Fu, S.H. Lian, C.L. Lin, C.L. Yang, An experimental investigation of a mixed convection in a ⊔ shape channel subject to a reciprocating motion, Int. J. Heat Mass Transfer 52 (2009) 3613–3627.
[16] Wärtsilä. <http://www.wartsila.com/.
[17] S.J. Kline, The purpose of uncertainty analysis, ASME J. Heat Transfer 117 (1985) 153–160.